ARTICLE

# Transitional Process of Ploy(N-isopropylacrylamide) in Deuterated Solution

Shao-hua Zhang[a], Yang Chen[a]*, Heng Li[b], Yu-xiang Weng[b]

*a. Hefei National Laboratory for Physical Sciences at the Microscale, Department of Chemical Physics, University of Science and Technology of China, Hefei 230026, China*
*b. Laboratory of Soft Matter Physics, Institute of Physics, Chinese Academy of Sciences; Beijing National Laboratory of Condensed Matter Physics, Beijing 100080, China*

(Dated: Received on June 11, 2009; Accepted on August 10, 2009)

The fast phase-transitional process of ploy(N-isopropylacrylamide) (PNIPAM) in deuterated solution was studied by laser induced temperature jump technique combined with time-resolved mid-infrared absorbance difference spectroscopy on nanosecond level. The multi-peaks of amide I′ band of PNIPAM among the energy range of 1565−1700 $cm^{-1}$ was experimentally resolved to three groups (i, ii, iii) for the first time, while the distinct three-stage procedure in the phase transitional process of long-chain PNIPAM was observed firstly too. Furthermore, proper assignments were also made for the three group peaks in amide I′ band and the three steps in the kinetics process of long-chain PNIPAM.

**Key words:** Poly(N-isopropylacrylamide), Laser induced temperature jump, Kinetic, Transient mid-infrared absorbance difference spectroscopy, Multistage, Transitional process

## I. INTRODUCTION

The phase transition of ploy(N-isopropylacrylamide) (PNIPAM) and its thermodynamic properties have been extensively explored by employing a wide variety of experimental techniques, *e.g.*, turbidity [1,2], light scattering [3,4], calorimetry [5,6], fluorescence [7,8], nuclear magnetic resonance [9], and static IR spectroscopy [10–12], etc. Up to date, abundant experiments have been carried out by many groups, but the phase transition of PNIPAM is still far from being understood comprehensively because of the absence of the efficient experimental techniques, especially the instruments of high resolution in time domain. Nevertheless, many models about the phase transition kinetics of PNIPAM during the temperature increasing process have been brought forward [13–19]. de Gennes and Grosberg *et al.* firstly presented a two-stage kinetics model in coil-to-globule transition [13,14]. However, based on the work published in Ref.[15], Kuznetsov *et al.* suggested that the coil-to-globule transitional process should contain at least four stages, *i.e.* the quick formation of small locally collapsed nuclei on the chain, the growth of these nuclei into clusters, the merging of these clusters to a globule, and the slow equilibration of a compact collapsed globule, etc. [16]. Then, Halperin *et al.* showed a similar four-stage phenomenological model [17] to characterize the process, wherein they called these four stages as: "pearling", "bridge stretching", "packing", and "merging", respectively. Recently, Estève *et al.* proposed that the coil of PNIPAM could form a local, self-saturated and well-ordered helix during the coil-to-globule transition process [18]. Kikuchi *et al.* predicted the initial "pearl" formation only took ∼5% of the overall transition time ($\tau$) even for a long chain [19].

Contrast to other methods of phase transition of PNIPAM, only a few experimental studies hitherto have been focused on the macromolecular phase transition kinetics in temperature jumping. Chu *et al.* observed the two-stage process with transition time about several minutes [20,21], and Kayaman *et al.* pointed that the transition time of first stage should be slower than 30 s [22]. Nakamura *et al.* indicated that the first stage of transition process is so short-lived that it is very difficult to be detected by their dynamic light scattering (DLS) spectrometer [23]. Liu *et al.* investigated the transition kinetics of copolymer (PNIPAM-co-pyrene) with the stopped-flow technique and found a two-stage process of which the character time parameters are $\tau_{\rm fast}$ of 12 ms and $\tau_{\rm slow}$ of 270 ms, respectively [24]. Recently, Ye *et al.* recorded a two-stage process of individual PNIPAM chains in dilute solutions in much shorter transition times scale ($\tau_{\rm fast}$≈0.1 ms, $\tau_{\rm slow}$≈0.8 ms) by fluorescence probe [25].

But all related experiments above just roughly measured movements of whole chains in the dilute solutions, and some of them complicated the problem further because of the additive reagents (hydrophobic fluorescence probes) in the PNIPAM solution. In this work, the kinetics process of each functional group of PNIPAM in real time was presented for the first time by using laser induced temperature jump technique combined with time-resolved mid-infrared (MIR) absorbance dif-

*Author to whom correspondence should be addressed. E-mail: yangchen@ustc.edu.cn

 

ference spectroscopy in nanosecond scale, excluding the interruptions of additive reagents completely.

## II. MATERIALS AND METHODS

The PNIPAM samples used were supplied by Wu group, and its synthesis process have been mentioned in detailed elsewhere [26]. The characteristic data of three functional groups of PNIPAM (1, 2, 3) employed in this work are summarized in Table I. In experiments, PNIPAM were dissolved in deuterated water with concentration of 2.0% and the solution was incubated for several days to complete the hydrogen-deuterium exchange sufficiently. Besides, PNIPAM-2 was further diluted to three other concentrations (0.75%, 1.0%, 1.5%).

TABLE I Laser light scattering characterization of PNIPAM samples used at 25.0 °C.

| Sample | $M_w$/(g/mol) | $R_g$/nm | $R_h$/nm | $M_w/M_n$ |
|---|---|---|---|---|
| PNIPAM-1 | $2.0\times10^4$ | 60 | 44 | 1.4 |
| PNIPAM-2 | $1.8\times10^6$ | 53 | 40 | 1.5 |
| PNIPAM-3 | $7.7\times10^6$ | 114 | 73 | 1.4 |

The laser induced temperature-jump (T-jump) technique and the time-resolved IR spectrometer have been described elsewhere [27]. Briefly, the fundamental output of a Nd:YAG laser (Lab 170, Spectra Physics) was introduced into a $H_2$-contained Raman cell (∼5 MPa) and generated the 1.9 μm laser as the heating source. A liquid $N_2$ cooled CW CO laser (Dalian University of Technology, Dalian) was employed as the IR probe source (tunable region: 2000–1540 $cm^{-1}$). The wavelength of the IR probe laser can be selected within the CO vibration-rotation spectra with a spectral spacing about 4 $cm^{-1}$, which was calibrated by an IR monochromator with uncertainty of 2 $cm^{-1}$. The IR probe beam was collected by a liquid $N_2$ cooled photovoltaic MCT detector (Kolmar, MA, USA) which is equipped with a sensitive current preamplifier (Kolmar, KA020-A1). The intensity of the transmitted IR probe beam and the corresponding transient absorbance change induced by the T-jump pulses were recorded by a digital oscilloscope (Tektronix TDS520D, Santa Clara, CA). The difference spectra were reconstructed by the optical difference between the T-jump induced absorbance change of the sample and that of the blank $D_2O$. The calibration of the T-jump amplitude follows the previously reported protocols [27]. In present work, the initial temperature was set at 28.9 °C and the average amplitude of T-jump is about 10 °C with the accuracy of the $\Delta T$ within ±1.5 °C. Under these conditions, it was guaranteed that the PNIPAM could change from coil to globule completely. The instrumental temporal response of this system was determined as ∼80 ns by fitting the T-jump kinetics of the $D_2O$ reference signal convoluted with a Gaussian instrumental response function, where the rising time for heating $D_2O$ is set as 20 ns based on the pulse width of the Q-switch Nd:YAG laser. A sample cell with two $CaF_2$ windows was employed in the T-jump measurement, which is divided by a 56 μm thick Teflon space into two parts. One compartment was filled with the sample solution and another with blank $D_2O$ as reference. The T-jump induced absorbance divergence was measured when the two compartments were both filled with $D_2O$, and the optical density (OD) was about $5\times10^{-4}$ after averaging for 300 laser shots while the OD difference between the sample and the reference was $5\times10^{-3}$–$1\times10^{-2}$.

## III. RESULTS AND DISCUSSION

The transient IR difference spectra of PNIPAM-2 (2.0%) in deuterated solutions with different time delay were shown in Fig.1 over the range of 1570–1700 $cm^{-1}$, including a static FTIR spectrum. These difference spectra were obtained from the absorbance spectra at higher temperature minus the corresponding ones at lower temperature. So, the plus peaks denote the absorbance peaks while the minus ones are the bleaching peaks. Obviously, in Fig.1, those transient spectra present five peaks (bleaching peaks: 1626, 1604, and 1595 $cm^{-1}$; absorbance peak: 1640 and 1646 $cm^{-1}$), while the static one merely presents a pair (bleaching peak: 1617 $cm^{-1}$, around 1625 $cm^{-1}$; absorbance one: 1642 $cm^{-1}$, around 1650 $cm^{-1}$), although they are similar in outlines. The wavelength of the static FTIR spectrum was calibrated as these transient ones.

In static FTIR spectrum, the peak around 1650 $cm^{-1}$ has been assigned to absorbance peak amide I or I′ (prime denotes the amides are deuterated). Owing to its sensitivity to hydrogen bonding, dipole-dipole interactions, and geometry of the peptide backbone, the

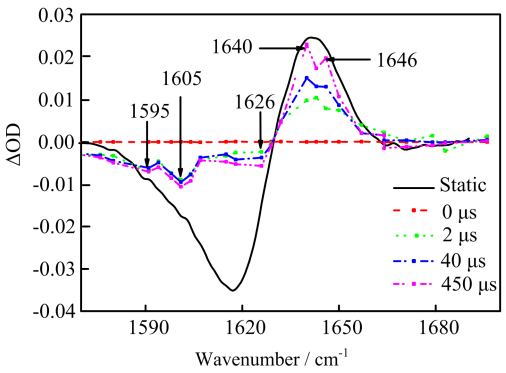


FIG. 1 IR difference absorbance spectra of PNIPAM-2 (2.0%). Four slices of the transient IR difference absorbance spectra on the different time after the coming of heating pulse were shown by different kinds of lines. The solid line is the static FTIR difference absorbance spectra of the same sample. The initial temperature was set at 28.9 °C and the average amplitude of T-jump is about 10 °C.

DOI:10.1088/1674-0068/22/05/447-452

amide I (or I′) infrared absorbance has become an established indicator for the secondary and tertiary structures of proteins or polymers. So the amide I (or I′) of PNIPAM has also been studied extensively and deeply. Maeda and his coworkers reported that when the temperature lower than its lower critical solution temperature (LCST, at ∼32 °C), the amide I′ band of PNIPAM consists of a single peak at about 1625 $cm^{-1}$ while above the LCST a new peak (1650 $cm^{-1}$ ) will appear [11]. They tentatively assigned the former peak to hydrogen bonding between the C=O group and water molecules, and the latter to the C=O group that form hydrogen bands with N−H groups and make intra- or interchain cross-linkages. However, Katsumoto *et al.* have provided the evidence for a contrary conclusion by DFT calculations combined with ATR/IR spectroscopy [28]. They believed that the ∼1626 $cm^{-1}$ band comes from the intramolecular C=O···D−N hydrogen bonding between the neighboring side chains of PNIPAM while the ∼1650 $cm^{-1}$ arises from the stretching vibration of the free C=O radicals. Recurring to pressure effect studying, Meersman *et al.* revealed the presence of two minor peaks at ∼1604 and ∼1653 $cm^{-1}$ of PNIPAM at 25°C and 0.1 MPa [29]. The former peak was suggested to result from the additionally C=O···D−O−D group while the latter one was assigned to non-hydrogen-bonded carbonyl. They also indicated that the ∼1626 $cm^{-1}$ peak arises from two kinds of hydrogen-bonded carbonyl: C=O···D−O−D and C=O···D−N conjointly. These two controversial assignments can help us to investigate the transition kinetics of PNIPAM in present work.

To study the transient IR spectra of PNIPAM, the kinetics plots of different peaks of the same PNIPAM were recorded in 1 μs time resolution and shown as different types of scatter-lines in Fig.2. All data were normalized to compare with each other. In Fig.2, we can see that the kinetic curve of the peak at 1640 $cm^{-1}$ is almost coincide with that of peak at 1646 $cm^{-1}$, and the same phenomenon also happens for the bleaching peaks of ∼1595 and ∼1605 $cm^{-1}$, although they are decaying. Based on the similar kinetics behavior, all peaks were naturally divided into three groups: the group i contains two absorbance peaks 1640 and 1646 $cm^{-1}$ ; the group ii is composed of two bleaching peaks 1595 and 1605 $cm^{-1}$; and the group iii has only a special bleaching peak at 1626 $cm^{-1}$. The peaks in the same group are determined to have the same kinetics behavior, which means that these peaks in the same group come from the same functional group. Fitting kinetics plots of three groups by a mono-exponential equation, the characteristic time constants in transition process of each group can be determined roughly, *i.e.* $\tau$ (group i): ∼80 μs; $\tau$ (group ii): ∼70 μs; and $\tau$ (group iii): ∼108 μs, respectively. So it can be suggested that these peaks of different groups (i–iii) corresponding to different functional groups go through different transition processes. By combining the assignments of peaks in the amide I′ of PNIPAM in Refs.[11,28], we attribute the 1626 $cm^{-1}$ peak to the intra- or intermolecular hydrogen bonding between the neighboring side chains of PNIPAM because of its slowest movement in all those peaks, and assign the other two bleaching peaks (1595 and 1605 $cm^{-1}$) to the intermolecular hydrogen bonding between the PNIPAM and the solvent $D_2O$ on account of their swiftest action. Moreover, the two absorbance peaks are certainly originated from the hydrogen-bond broken or dehydrated during the transition process.

In order to validate the new assignment of the amide I′ band of PNIPAM, the solution concentration of PNIPAM-2 was varied from 0.5% to 2%. The dependence of character transition times on solution concentrations for typical peaks (1605, 1626, and 1646 $cm^{-1}$) was displayed in Fig.3. The lifetime of transitional process of the peak at 1626 $cm^{-1}$ which was assigned to intra- or interchain cross-linkage increases linearly with the concentration rising. It is easy to understand that the dehydration of higher concentration solution is harder than the thinner one in the transition process, because higher concentration can induce much more intra- or interchain hydrogen bonds in solution below the LCST. Therefore, the assignment of the 1626 $cm^{-1}$ peak was pinpointed as intra- or interchain hydrogen-bond cross-linkage between neighboring side chains of

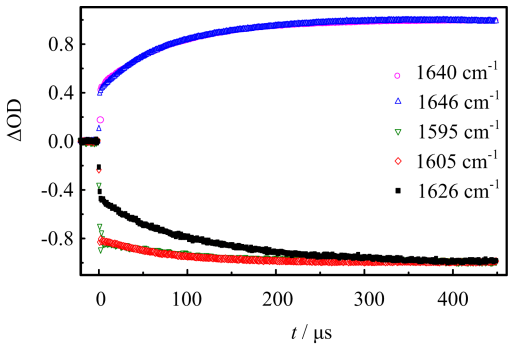


FIG. 2 Kinetic curves of different peaks in amide I′ of PNIPAM-2 (2.0%). Data has been normalized.

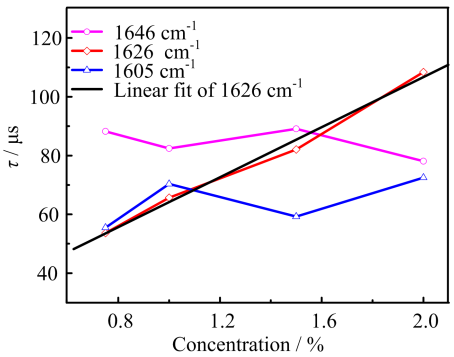


FIG. 3 Concentration dependence of characteristic transitional time constants of typical peaks of PNIPAM-2.

DOI:10.1088/1674-0068/22/05/447-452

PNIPAM. Under the influence of near hydrogen bonds, the frequency of the carbonyl C=O bond will red shift by reducing reducing its electron density, thus we can attributed peaks at 1640 $cm^{-1}$ and 1646 $cm^{-1}$ to dehydrated hydrogen-bonded carbonyl (free C=O) during the transition process. Consequently, the bleaching peaks (1605 and 1595 $cm^{-1}$) can be assigned to hydrogen-bonded carbonyl with water.

To display the multistage procedure of peaks in transition process more clearly, the semi-logarithmic plot of (1-ΔOD) *vs.* $t$ (ΔOD is the difference optical density of the certain peak) was figured from the kinetic curve of the 1646 $cm^{-1}$ peak of PNIPAM-2 (2.0%) which has been demonstrated in Fig.2 and presented in Fig.4.

As shown in Fig.4, the three steps with different timescales, denoted by step I, step II, and step III, respectively, were presented rather distinctly. Along the transition curve, the part from the initial time zero to 2 μs is step I; the following 2–380 μs is step II and the left belongs to step III which is rather conspicuous because of its inverted route. By the way, it is the semilogarithmic plot of the kinetic curve, so the data before $t$=0 is the semi-logarithmic of zero and means nothing. The kinetic plot of the 1646 $cm^{-1}$ peak was fitted exactly by a third-order exponential equation and three characteristic transition time constants ∼1.32, ∼78.12, and ∼−3000 μs (negative means this step is inverted), were obtained, in which the lifetime of step II is almost equal to the roughly characteristic transition time constants of whole transition process mentioned above. Because roughly time constants are related to functional groups of PNIPAM molecule, it can be deduced that the lifetime of step II depends on the functional groups of PNIPAM. To confirm this deduction, the semilogarithmic plots of 1626 and 1646 $cm^{-1}$ peaks of the same PNIPAM were selected out and exhibited in Fig.5. The quite big divergence between the two steps II of two peaks was presented, however, there is no noticeable difference between steps of I and III. These facts not only verified the deduction above but also confirmed our previous assignments again. And they also provided us the information that time constants of the step III are not related to functional groups of PNIPAM, hence the step III represents the movements of whole chain of PNIPAM but not some location. Besides, the inverted route of the step III means that, in this period, the PNIPAM molecular has revived already.

As discussed above, all experimental data were recorded with 1μs time resolution, so the step I is too fast to be resolved precisely in occurrence time resolution and needs more exploration in higher time resolution. In Fig.6, we showed the typical semilogarithmic plot of peak 1646 $cm^{-1}$ of PNIPAM-2 (2.0%) which was figured from the kinetic curve recorded in 10 ns time resolution. The whole plot corresponds to the step I of the plot shown in Fig.4. Similarly, the plot can be divided to new three steps: a, b, and c, and the corresponding time constants are ∼86 ns, ∼920 ns, $+\infty$, respectively, by fitting the plot with a third order exponential equation. Considering the known lifetime of the step II and the time resolution (10 ns), we believe that the unreasonable lifetime of the step c is owing to inaccurate ex-

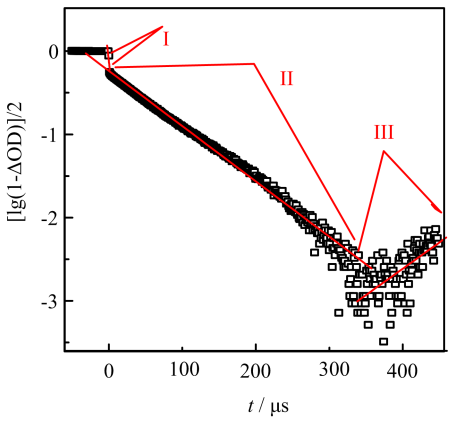


FIG. 4 A typical semilogarithmic plot of (1–ΔOD) *vs.* $t$. ΔOD is the difference optical density of the peak at 1646 $cm^{-1}$ of PNIPAM-2 (2.0%). I, II, and III show different timescales.

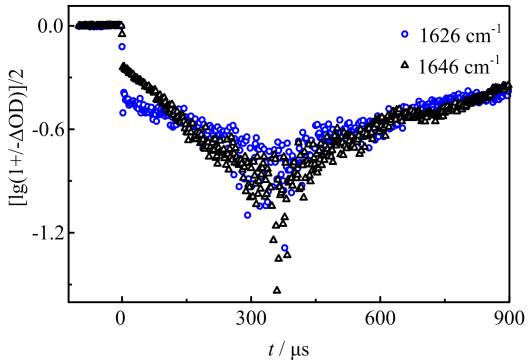


FIG. 5 Semilogarithmic plots of (1–ΔOD) *vs.* $t$ of different peaks of PNIPAM-2 (2.0%, 1626 and 1646 $cm^{-1}$).

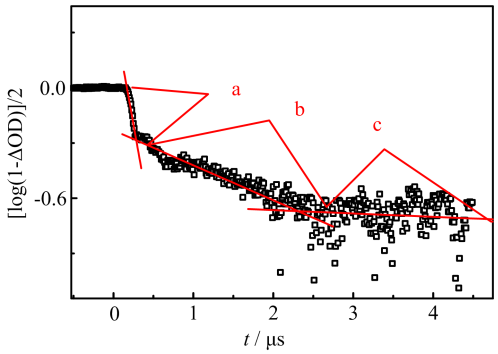


FIG. 6 The semilogarithmic plots of (1-ΔOD) *vs.* $t$ of the peak at 1646 $cm^{-1}$ of PNIPAM-2 (2.0%) which was figured from the kinetic curve recorded in 10 ns time resolution. a, b, and c show three different steps.

DOI:10.1088/1674-0068/22/05/447-452

pression of the step II in Fig.4. The step a ($\tau \approx 86$ ns) should originate from the heating pulse convolved by the instrumental response function, which matched the fact that the instrumental temporal response of this experimental system (80 ns) as mentioned above. So, the step b in Fig.6 is homologous to the step I in Fig.4.

The fast activities of different peaks of PNIPAM with different concentrations were measured with 10 ns time resolution and they are similar to each other. The differences between time constants of different peaks are unnoticeable and the relationship between lifetimes of step b and the concentrations for all peaks in amide I′ are totally irregular. So, the step I is irrelevant to functional groups of PNIPAM and also independent of the concentration.

The influences of chain length on the kinetics processes are also explored in our experiments. Three different kinds of PNIPAM (1, 2, 3) (2.0%) were involved. The semilogarithmic plots of peaks 1646 $cm^{-1}$ of the three PNIPAM were shown in Fig.7. According to Fig.7, the multistage procedures in transition process occur on the long-chain PNIPAM while the only one stairstep happens on the semi-logarithmic plot of the short-chain PNIPAM. It means that there is no any long-time changed procedure in the short-chain PNIPAM transition process. So, it was concluded that the slower steps (step II and step III) are related to the long-chain PNIPAM only. Besides, our studies on the step I (not shown) of these three kinds of PNIPAM in 10 ns of time resolution also showed that lifetimes of step I are independent of the chain length.

As all these experimental results are consistent with the predictions in the Refs.[16,17] perfectly. Step I was contributed to the quick formation of small locally collapsed nuclei on the chain which was defined by Kuznetsov *et al.* [16], as its time constants ($\sim$1 μs) are independent of functional groups, concentration and chain length; while step II ($\tau \approx 80$ μs) was assigned as the growth of these nuclei into clusters because its lifetimes are related to functional groups, chain length, and concentration (for the special peak); and the inverted step III was assigned as a compulsively inverted transition process originated from the thermal relaxation process of this experimental system, due to its relationship with the chain length and independence of functional groups and the relatively longer lifetime ($\sim$3 ms) which quite close to the decay time of the thermal relaxation of this experimental system ($\sim$6 ms).

## IV. CONCLUSION

The transient time-resolved IR difference spectroscopy of PNIPAM in deuterated solution in the spectrum range of 1570–1700 $cm^{-1}$ was recorded and analyzed for the first time. The IR peaks in amide I′ band were resolved to three groups (i, ii, iii) and assigned as intra- or interchain hydrogen-bond crosslinkage in PNIPAM molecular; hydrogen-bonded carbonyl with water and dehydrated hydrogen-bonded carbonyl (free C=O) respectively. Furthermore, the time-resolved kinetics of typical peaks which correspond to different functional groups in PNIPAM molecule was also firstly investigated in experiment. A distinct three-stage procedure in the transitional process of long-chain PNIPAM was observed and the three steps were attributed to the quick formation of small locally collapsed nuclei on the chain; the growth of these nuclei into clusters and a compulsively inverted transition process induced by the thermal relaxation process respectively.

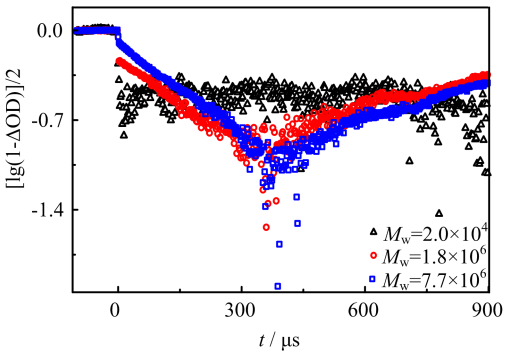


FIG. 7 Semilogarithmic plots of (1–ΔOD) *vs.* $t$ of the peak at 1646 $cm^{-1}$ of three different chain-length PNIPAM(1,2,3) (2.0%).

## V. ACKNOWLEDGMENTS

This work was supported by the National Natural Science Foundation of China (No.20673107), the National Key Basic Research Special Foundation of China (No.2007CB815203), and the Knowledge Innovation Foundation of the Chinese Academy of Science (No.KJCX2-SW-H08).

[1] M. Heskins and J. E. Guillet, J. Macromol. Sci. Chem. **A2**, 1441 (1968).
[2] S. Fujishige, K. Kubota, and I. Ando, J. Phys. Chem. **93**, 3311 (1989).
[3] K. Kubota, S. Fujishige, and I. Ando, J. Phys. Chem. **94**, 5154 (1990).
[4] X. Wan, X. Qiu, and C. Wu, Macromolecules **31**, 2972 (1998).
[5] H. G. Schild and D. A. Tirrell, J. Phys. Chem. **94**, 4352 (1990).
[6] H. Inomata, S. Goto, K. Otake, and S. Saito, Langmuir **8**, 687 (1992).
[7] F. M. Winnk, Macromolecules **23**, 233 (1990).
[8] R. Walter, J. Rièka, C. Quellet, R. Nyffenegger, and T. Binkert, Macromolecules **29**, 4019 (1996).
[9] H. Ohta, I. Ando, S. Fujishige, and K. Kubota, J. Polym. Sci. Polym. Phys. Ed. **29**, 963 (1991).

DOI:10.1088/1674-0068/22/05/447-452 

[10] A. Percot, X. X. Zhu, and M. Lafleur, J. Polym. Sci. Polym. Phys. Ed. **38**, 907 (2000).
[11] Y. Maeda, T. Higuchi, and I. Ikeda, Langmuir **16**, 7503 (2000).
[12] Y. Maeda, T. Nakamura, and I. Ikeda, Macromolecules **34**, 1391 (2001).
[13] P. G. de. Gennes, J. Phys. Lett **46**, L639 (1985).
[14] A. Y. Grosberg, S. K. Nechaev, and E. I. Shakhnovich, J. Phys. France **49**, 2095 (1988).
[15] A. Byrne, P. Kiernan, D. Green, and K. A. Dawson, J. Chem. Phys. **102**, 573 (1995).
[16] Y. A. Kuznetsov, E. G. Timoshenko, and K. A. Dawson, J. Chem. Phys. **104**, 3338 (1996).
[17] A. Halperin and P. M. Goldbart, Phys. Rev. E **61**, 565 (2000).
[18] A. Estève, A. Bail, G. Landa, A. Dkhissi, M. Brut, M. D. Rouhani, J. Sudor, and A. M. Gué, Chem. Phys. **340**, 12 (2007).
[19] N. Kikuchi, J. F. Ryder, C. M. Pooley, and J. M. Yeomans, Phys. Rev. E **71**, 061804 (2005).
[20] B. Chu, Q. C. Ying, and A. Y. Grosberg, Macromolecules **28**, 180 (1995).
[21] B. Chu and Q. C. Ying, Macromolecules **29**, 1824 (1996).
[22] N. Kayaman, E. E. Gürel, B. M. Baysal, and F. E. Karasz, Macromolecules **32**, 8399 (1999).
[23] Y. Nakamura, N. Sasak, and M. Nakata, Macromolecules **34**, 5992 (2001).
[24] J. Xu, Z. Y. Zhu, S. Z. Luo, C. Wu, and S. Y. Liu, Phys. Rev. Lett. **96**, 027802 (2006).
[25] X. D. Ye, Y. J. Lu, L. Shen, Y. W. Ding, S. L. Liu, G. Z. Zhang, and C. Wu, Macromolecules **40**, 4750 (2007).
[26] C. Wu and S. Q. Zhou, Macromolecules **28**, 8381 (1995).
[27] M. P. Ye, Q. L. Zhang, H. Li, Y. X. Weng, W. C. Wang, and X. G. Qiu, Biophys. J. **107**, 106799 (2007).
[28] Y. Katsumoto, T. Tanaka, and Y. Ozaki, Macromol. Symp. **205**, 209 (2004).
[29] F. Meersman, L. Smeller, and K. Heremans, Biophys. J. **82**, 2365 (2002).

DOI:10.1088/1674-0068/22/05/447-452 